Astron. Astrophys. 318, 376–382 (1997)

ASTRONOMY AND ASTROPHYSICS

The radio source OQ 208: parsec-scale morphology and spectral properties

C. Stanghellini[1,7], **M. Bondi**[2,3], **D. Dallacasa**[2,4], **C.P.O'Dea**[5], **S.A. Baum**[5], **R. Fanti**[2,6], **and C. Fanti**[2,6]

[1] Istituto di Radioastronomia del CNR, C.P. 141, I-96017 Noto SR, Italy
[2] Istituto di Radioastronomia del CNR, Via Gobetti 101, I-40129 Bologna, Italy
[3] Nuffield Radio Astronomy Laboratories, Jodrell Bank, Macclesfield, Cheshire, SK11 9DL, UK
[4] Joint Institute for VLBI in Europe, Postbus 2, 7990 AA Dwingeloo, The Netherlands
[5] Space Telescope Science Institute, 3700 San Martin Drive, Baltimore, MD, 21218
[6] Dipartimento di Fisica, Università degli Studi, via Irnerio 46, I-40126 Bologna, Italy
[7] Visitor at the Space Telescope Science Institute, Baltimore.

Received 19 December 1995 / Accepted 22 July 1996

Abstract. We present results from global VLBI (Very Long Baseline Interferometry) observations at 5 GHz of the radio source OQ 208. The milliarcsecond (mas) morphology of the radio emission is described by an asymmetric compact double structure with a flux density ratio between the two components of about 10:1, and a projected total size of $\sim$ 7 mas (i.e. $\sim$ 7 pc). Both components are resolved by the present observations.

Multifrequency VLA (Very Large Array) observations are used to define the spectral shape and, together with literature data, to investigate the flux density variability at different frequencies. The integrated radio spectrum is peaked at about 4 GHz. The flux density is constant below the peak and slowly decreasing at frequencies above the peak.

On the basis of the mas morphology, spectral information and flux density variations, we favour the hypothesis that the radio source consists of two parsec-size lobes undergoing synchrotron radiative losses.

Key words: galaxies: OQ 208=Mkn 668 – galaxies: active – radio continuum: galaxies

1. Introduction

OQ 208 (1404+286) is a compact radio source associated with the bright galaxy Mkn668 of m_r=14.6 (Stanghellini et al. 1993) at z = 0.077 (Burbidge and Strittmatter 1972). This object has been often classified as a Seyfert 1 galaxy. However, due to its strong radio emission we prefer the classification of Broad Line Radio Galaxy (BLRG) (Marziani et al. 1993).

Its optical properties are quite peculiar. Marziani et al. (1993) have observed very complex Balmer line profiles which are supposed to reflect the geometrical structure and kinematics in the Broad Line Region (BLR). Their favoured explanation for these line profiles involves outflow of emitting gas radiatively accelerated in a biconical geometry, and emission from clouds spherically distributed.

The optical image presented by Stanghellini et al. (1993) shows the presence of companions in the galactic envelope and a tail of low brightness emission in N-S direction, suggesting that the galaxy is dynamically disturbed.

Granato et al. (1993) fit the optical intensity profile with the contribution of an unresolved nucleus, responsible for approximately half of the optical emission, and a disk galaxy.

OQ 208 is the closest known example of bright GHz-Peaked-Spectrum (GPS) radio source (O'Dea et al. 1991), making it the best target for a high linear resolution investigation of this class of compact objects. The redshift of OQ 208 locates the source at a distance of $\sim$ 240 Mpc (we use H_0 = 100 km s^{-1} Mpc^{-1}) and 1 mas corresponds to about 1 pc.

The radio source OQ 208 has been often used as a VLBI (Very Long Baseline Interferometry) calibrator due to its compactness. However, at 5 GHz the source has been found to be resolved on baselines $> 15\ M\lambda$ by Bondi et al. (1994).

VLBI observations of OQ 208 were first carried out by Matveenko et al. (1981) and Zensus et al. (1984). These early observations were interpreted in terms of a single Gaussian component model. At 1.6 GHz, Matveenko et al. (1981) found that the structure of OQ 208 is extended in p.a. -120°, whereas, at 5 GHz, Zensus et al. (1984) found that it is extended in the N-S direction (p.a. -8°). The first published VLBI image of OQ 208 (Charlot 1990) confirmed the N-S extension, indicating that the structure of OQ 208 at 8.4 GHz consists of two components separated by $\sim$ 1.3 mas at p.a. -15°. The variation in position angle from the highest frequency (8.4 GHz) to the lowest frequency (1.6 GHz) has been interpreted in terms of a highly curved jet

Send offprint requests to: C. Stanghellini

Table 1. Antennas involved in the VLBI experiment. The nominal system equivalent flux density (SEFD) in column 3 is given by the ratio between the system temperature (in K) and the antenna gain (in K/Jy).

Antenna	Diam. (m)	nominal SEFD (Jy)
Onsala (Swe)	20	990
Bonn (Ger)	100	44
WSRT (Ned)	93	107
JBNK2 (UK)	25	344
Medicina (Ita)	32	290
Noto (Ita)	32	194
NRAO (US)	43	130
VLBA-KP	25	300
VLBA-PT	25	300
VLBA-NL	25	300
VLBA-BR	25	300
VLBA-OV	25	300
VLBA-SC	25	300
VLBA-HN	25	300
VLA	25	330

where different parts are visible at different frequencies. Later images at 1.6 and 5 GHz by Bondi et al. (1994) and Zhang et al. (1994) revealed the presence of an additional weak component ∼6 mas in the S-W direction, corresponding probably to the extension in p.a. -120° first detected by Matveenko et al. (1981) at 1.6 GHz. The observations of Zhang et al. (1994) also indicate that the dominant component is elongated along the N-S direction, in agreement with the previous results by Zensus et al. (1984) and Charlot (1990). From their 1.6 and 5 GHz data, Zhang et al. (1994) interpret the observed morphological structure as a core-jet, typical of the compact flat-spectrum radio sources. In this paper, we reinterpret the radio structure of OQ 208 based on a new 5 GHz map with improved dynamic range and resolution, supplemented with VLA (Very Large Array) data.

2. Observations and data reduction

The 5 GHz observations were carried out in February 1993 as part of a project studying a sample of GPS radio sources (Stanghellini et al., in preparation) using a global VLBI network at 4.992 GHz and the MK II recording system (Clark 1973). The list of antennas is given in Table 1. OQ 208 was observed in four 30-minute scans with the complete global array, and in two scans with the European and American antennas separately. These snapshots, over a range of hour angles, gave the uv coverage shown in Fig. 1.

The data were correlated at the Caltech/JPL Block II correlator. The Astronomical Image Processing System (AIPS) developed by the National Radio Astronomy Observatory (NRAO), has been used for editing, initial calibration, fringe-fitting, imaging and self-calibration. After the application of the *a-priori* amplitude calibration, the data passed through several iterations of phase self-calibration, then a final iteration of amplitude and phase self-calibration. The flux density scale was calibrated using the compact radio sources 0016+731, 0235+164, and DA193, with adopted flux densities of 1.71 Jy, 3.97 Jy, and 6.95 Jy respectively as measured at Effelsberg and/or at the Westerbork Synthesis Radio Telescope (WSRT) during the same VLBI session.

Table 2. Log of VLA observations

Epoch	ν_{GHz}	config.
11 Jun 89	1.665	C
09 Feb 90	1.380	A
09 Feb 90	1.630	A
11 Oct 94	4.850	B→C
11 Oct 94	8.540	B→C
21 Feb 95	14.940	D
21 Feb 95	22.460	D

Additional VLA snapshots obtained in several sessions have been considered in order to study the spectral shape. In general these data have been obtained in experiments where OQ 208 was used as a phase calibrator. Longer observations were available in A and C configuration at 1.6 GHz. These latter data were imaged independently and combined to look for any presence of low brightness diffuse emission around the strong compact component. The log of the VLA observations is given in Table 2. All the VLA data have been analyzed in AIPS for editing and calibration. Imaging and self-calibration has been performed for the data at 1.6 GHz in the A and C configurations mentioned before.

Additional flux density measurements from literature were used to extend the time and frequency coverage.

3. Results

3.1. The parsec scale morphology

OQ 208 is still used as a calibrator source in many VLBI experiments. The visibility plot (Fig. 2) clearly shows that the source is resolved at 5 GHz on baselines larger than 15-20 Mλ ($\sim$ 1000 km), therefore it is not a suitable calibrator at least in this observing frequency for standard EVN (European VLBI Network), VLBA (Very Long Baseline Array) or global VLBI observations. The image at 5 GHz restored with a Gaussian beam of the size of the central lobe of the dirty beam (1.6 × 0.8 mas in p.a. -11°) is shown in Fig. 3a. The main component is resolved in N-S direction; at $\sim$ 7 mas in p.a. $\sim -120°$ there is a secondary component resolved in two sub-components.

On the basis of the good uv-coverage and the high S/N ratio on all the baselines, we decided to create a slightly super-resolved image restoring the clean components with a circular Gaussian beam of 1 mas obtaining a better evidence of the com-

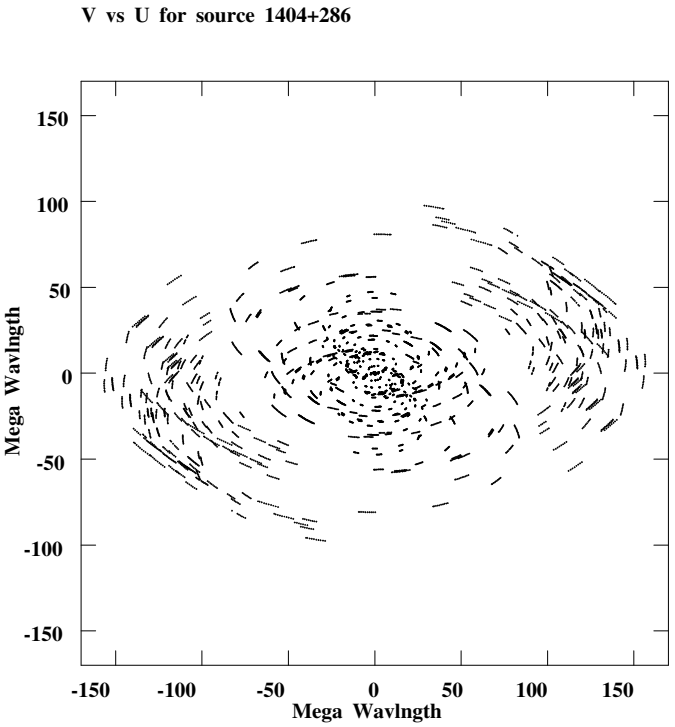

Fig. 1. UV-coverage of the observation.

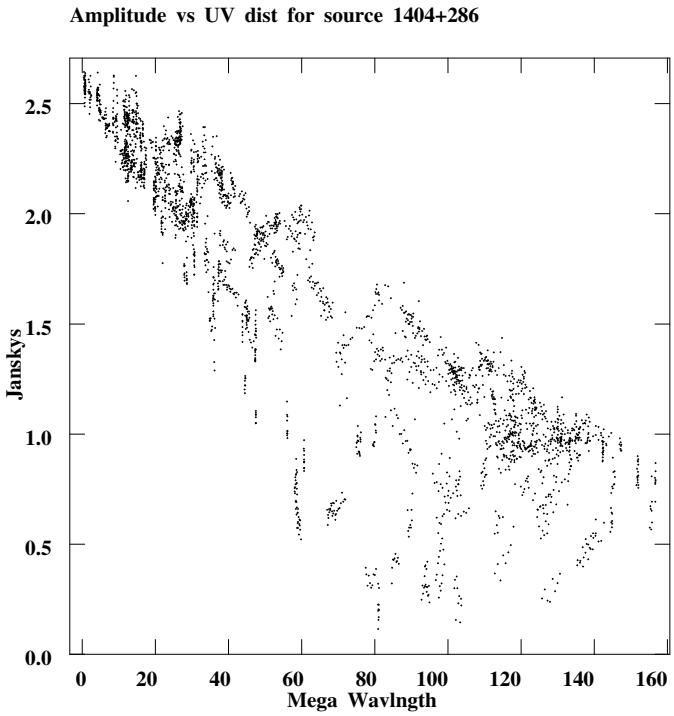

Fig. 2. Amplitudes versus baseline length from the 5 GHz observation of OQ 208

Table 3. Model fitting parameters.

Comp.	Flux Density (Jy)	r (mas)	ϕ (°)	θ (mas)
A	1.25 ± 0.03	0	0	1.2 ± 0.1
B	1.09 ± 0.03	1.3 ± 0.1	-14 ± 2	1.7 ± 0.2
C	0.10 ± 0.03	6.5 ± 0.1	-121 ± 4	2.2 ± 0.3
D	0.11 ± 0.03	7.4 ± 0.1	-117 ± 4	0.8 ± 0.3

Table 4. Physical parameters

Comp.	u_{min} (erg cm^{-3})	H_{eq} (gauss)	ν_{sa} (GHz)	τ (yr)
A	7.5×10^{-4}	9.0×10^{-2}	4.5	25
B	3.8×10^{-4}	6.4×10^{-2}	3.3	45
C	6.3×10^{-5}	2.6×10^{-2}	1.2	160
D	3.7×10^{-4}	6.4×10^{-2}	2.6	45

plex structure of the source (Fig. 3b). In this image the dominant component itself is resolved into an elongated structure in p.a. $\sim -15°$ which can be fitted with two components separated by 1.3 mas, in agreement with the image published by Charlot (1990) at 8.4 GHz. The superesolution is indeed along the structure of the stronger emitting region, but the brightness of several hundreds of mJy per beam and the modest superesolution factor (1.6) should guarantee the reliability of the morphology seen.

In order to derive the physical parameters we fitted both the image and the uv-data with four spherical components using the JMFIT task in AIPS and the MODELFIT task in the Caltech VLBI package, obtaining similar results. We preferred to use spherical instead of gaussian components because the former ones are used in the usual formulae of equipartition. Gaussian FWHM (Full Width Half Maximum) can be derived from the angular size of the spherical component divided by 1.8 (Marscher 1977). The flux density (Jy), distance r (mas) and position angle ϕ (°) from a reference position, and angular sizes θ (mas) of each component are shown in Table 3. The errors quoted in Table 3 have been estimated considering the differences between the various possible models minimizing the agreement factors. The error on the flux densities does not include the a-priori amplitude calibration error which we estimate to be about 5%.

The distance and position angle of components C and D are consistent with the results presented by Bondi et al. (1994) based on observations carried out in 1987, while Zhang et al. (1994) observed OQ 208 in 1990 and derived smaller distances and slightly different position angles. However, the model of Zhang et al. (1994) includes only three components (A+B, C, D), thus it is extremely risky to deduce possible structural variations and proper motions based on this comparison.

3.2. The flux density variability

Several flux density measurements of OQ 208 at 1.6 and 5 GHz spanning ∼15 years are presented in Fig. 4. The data are taken either from the literature or from our VLA observations.

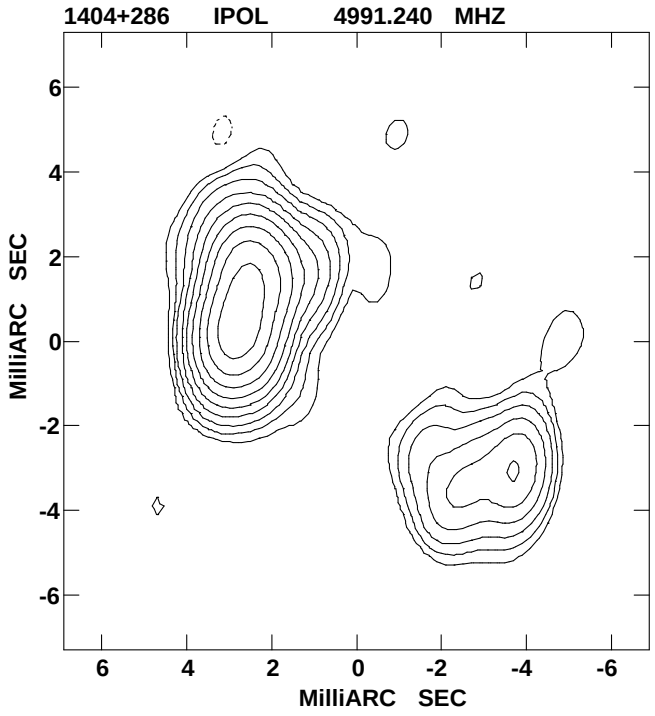

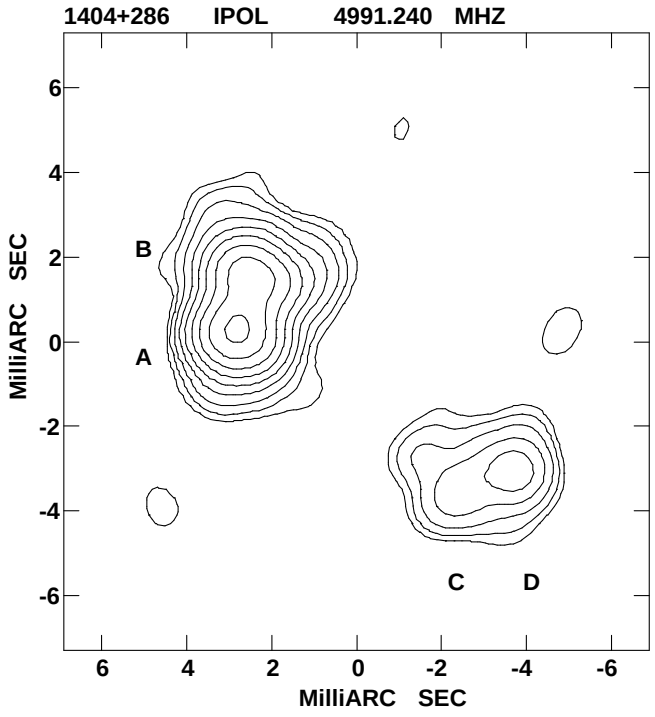

Fig. 3. a 5 GHz image of OQ 208: the beam is 1.6×0.8 mas in p.a. -11°, contour levels are -3, 3, 6, 12, 25, 50, 100, 200, 400, 800 times the noise of 0.8 mJy/beam, the peak flux density is 1106 mJy. **b** 5 GHz image convolved with a circular Gaussian beam of 1 mas, contour levels are as above, the noise is 1.0 mJy/beam, the peak flux density is 945 mJy.

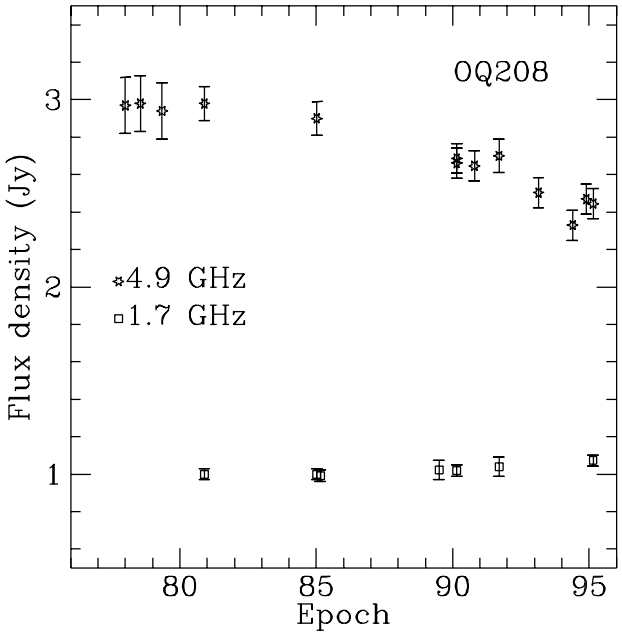

Fig. 4. Flux density measurements at 1.6 and 5 GHz (our data and from the literature: Perley 1982, Rusk 1988, Murphy 1988, Dallacasa et al. 1995, Stanghellini et al. in preparation, Foley private communication, Owen et al. 1980, Umana private communication, Kühr et al. 1981.)

The flux density is decreasing at 5 GHz but is constant at 1.6 GHz (Fig. 4). This confirms the results by de Bruyn (1990a,b) who claims that the source flux density has been stable at 1.4 GHz from 1979 to 1990 at a level of less than 0.2% per year, while it has decreased by about 10% at 5 GHz from 1977 to 1988.

OQ 208 has been monitored in the past years at 2.7 and 8 GHz with the Green Bank interferometer (Waltman et al. 1991; Waltman, private communication). The flux density in the S radio band (the observing frequency was 2.7 GHz from mid 1983 to mid 1989, and then 2.2 GHz from mid 1989 onwards) has been found to be stable, with all the data within 3 % of the mean value (at each frequency). Conversely, in the X radio band Waltman et al. (1991) observed a decrease of the flux density from about 2.7 Jy in mid 1983 to about 2.0 Jy in mid 1989 (observing frequency of 8.1 GHz). From mid 1989 onwards the receiver has been tuned to 8.3 GHz and the flux density has been found to be nearly constant around 1.9 Jy.

3.3. The integrated spectrum

The recentmost VLA data have been used to derive the spectrum shown in Fig. 5 with additional data from Mingaliev (private communication) and from the literature. All the data at frequencies higher than the turnover frequency have been taken between October 1994 and February 1995, so that variability should have only a marginal influence on the total spectrum.

The spectral index (where $S_\nu \propto \nu^\alpha$) is $\alpha \simeq -1.1$ between 8.4 and 15 GHz and steepens to $\alpha \simeq -1.7$ between 15 and 22

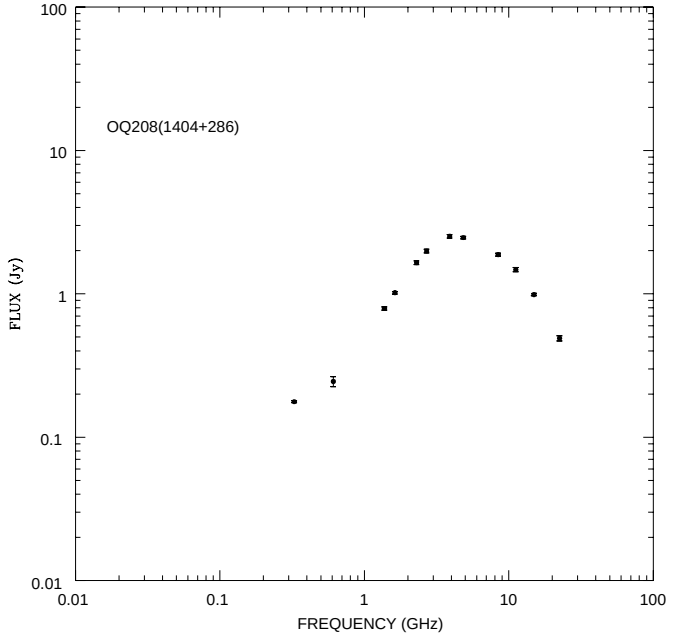

Fig. 5. The integrated spectrum of OQ 208. VLA measurements at 22, 15, 8.4, 5, 1.6, 1.4 GHz (Sect. 2); de Bruyn 1990a at 0.3 GHz and private communication at 0.6 GHz, Mingaliev private communication at 2.3, 3.9 and 11.2 GHz, Waltman et al. 1991 at 2.7 GHz.

GHz. The spectrum peaks at about 4 GHz, the index is $\alpha \simeq 1.5$ around 1 GHz and then flattens again below 0.6 GHz.

WSRT data at 5 GHz show a weak (6 mJy) and extended (20") radio halo (van der Laan et al. 1984; de Bruyn 1990a) around the compact object which could represent the contribution of the disk of the galaxy (or a weak lobe). In fact its N-S extension reflects the morphology and size seen in the optical image presented by Stanghellini et al. (1993) and its luminosity of $\sim 6 \times 10^{22}$ W/Hz is in the range of radio luminosity, $10^{18} - 10^{23}$ W/Hz, observed in normal spiral galaxies (Condon 1992). If we assume a steep spectral index $\alpha \sim$ -1 for the extended emission, this halo could be responsible for the flattening of the integrated spectrum at low frequencies. However, from our VLA snapshot observations in the A+C configuration at 1665 MHz (with a resolution of about 1.5 arcsecond) we do not detect any significant emission at 0.06 mJy/arcsec^2 level. More sensitive observations are needed to confirm or rule out the existence of the radio halo.

4. Discussion

The sharp peak in the spectrum of OQ 208 is consistent with the possibility that the VLBI components have similar spectral shapes. Furthermore the N-E and S-W components despite their difference in flux density appear to be morphologically similar and have comparable sizes.

As stated by de Bruyn (1990a,b) the lack of variability of the optically thick part of the spectrum implies that the source is strongly confined, because any adiabatic expansion would lead to a decrease in opacity and an *increase* in the flux density at 1.4 GHz. The case may be more complex if we consider a continuous supply of energy to the emitting region, but in any case the decrease in flux density at 5 GHz and the extreme stability at 2.7/2.2 GHz (Waltman et al. 1991), at 1.6 GHz (Fig. 4) and at 1.4 GHz (de Bruyn 1990a,b) is not consistent with simple adiabatic expansion of the radio source. We suggest that the decrease in flux density at 5 GHz (where the source is presumably becoming optically thin) is due mainly to radiative losses rather than to adiabatic expansion.

The flux density variation at 8.1/8.3 GHz may be a problem since the decrease has stopped from mid 1989 onwards, while it is continuing at 5 GHz. Different regions in the radio source might have different time scales for radiative losses, due to localized strong magnetic fields, causing the different flux density variations observed at 5 GHz and 8 GHz. The present data do not allow us to investigate this aspect in more details.

In Table 4 for each component we show the minimum energy density (u_{min}, in column 2) and the equipartition magnetic field (H_{eq}, in column 3) calculated with the parameters derived from model fitting. The equipartition magnetic field has been considered to derive the turnover frequency (ν_{sa}, in column 4), and the life time of the electrons radiating at 5 GHz (τ, in column 5). The common equations (e.g. Pacholczyk 1970) have been used, with the assumption of four homogeneous spherical region radiating by incoherent synchrotron emission, and a spectral index of -0.8.

We note that the turnover frequencies and life times of the electrons of the two dominant components A and B are in agreement with the integrated spectral properties of the source and its variability properties. In fact, the observed turnover frequency of the overall spectrum is intermediate between the calculated turnover frequency of components A and B, and the life time of the electrons at 5 GHz is compatible with the observed variability.

This is consistent with the underlying assumptions being roughly correct, i.e. the source is close to the equipartition, the turnover in the spectrum is due to synchrotron self-absorption, and the flux density decrease at 5 GHz is due to radiative losses. The combined evidence that in the optically thin region the flux density is decreasing and the spectrum progressively steepens at higher frequencies suggests that the eventual resupply of fresh electrons does not balance the ageing of the old ones.

The extreme stability of the radio flux at 1.4 GHz can be used to put a severe constraint on the expansion velocity of the source. The upper limit to a variation of the flux density of OQ 208 at 1.4 GHz is 0.2% per year. If we conservatively ascribe this variation to the strongest component of approximately half the flux density of the entire radio source, the limit in the percentage of the decrease becomes 0.4% per year.

We estimated for this component a radius of ~ 0.6 mas (i.e. 0.6 pc) for a homogeneous spherical model.

At 1.4 GHz we are in the optically thick part of the spectrum and the radio emission comes from the external layers of the radio source. Then the flux density S is related to the size r of the emitting region and to the magnetic field B by the relation $S \propto r^2 B^{-1/2}$ (Marscher 1977). Assuming adiabatic expan-

sion $B \propto r^{-2}$ then $S \propto r^3$, but in our case we probably have injection of new electrons and the expansion is not adiabatic. Then the magnetic field has presumably a weaker dependence from the radius, and S scales approximately with the solid angle subtended by the radio source i.e. r^2 rather than r^3 (de Bruyn 1990b). Therefore the limit of 0.4% per year in the increase of the flux density of the radio source becomes a limit of 0.2% per year in the increase of the radius. For the radius of 0.6 mas (0.6 pc) estimated for component A (see Table 3), this corresponds to an upper limit of the expansion velocity of $\sim$ 1200 km/s (that would be $\sim$ 800 km/s in the case of adiabatic expansion), in agreement with the value of 1000 km/s estimated by de Bruyn (1990b). This upper limit for the expansion velocity is also consistent with the predictions of the "jet-fed bubble" model for GPS sources (Bicknell et al. 1996).

If the radio source (the strongest component) is confined by ram pressure ($P = Nm_pv^2$, where P is $\frac{13}{21}\ u_{min}$, N is the particle density, m_p is the mass of the proton, and v is the expansion speed; see Pacholczyk, 1970), the forementioned limit on the expansion velocity (1200 km/s) and the equipartition energy densities u_{min} given in Table 3 (7.5×10^{-4} erg cm^{-3}) can be used to obtain a lower limit for the external particle density, which is N$> 2 \times 10^4$cm^{-3}, an order of magnitude higher than the typical density of a Narrow Line Region (NLR) cloud. Indeed, with an extent of a few parsecs OQ 208 is outside the BLR, but closer to the center of activity than an "average" NLR cloud. If the confining cloud has a high ionization fraction f, then free-free absorption may be significant. For example, given the density estimate of N$> 2 \times 10^4$cm^{-3}, a path length of 1 pc, and a temperature of 10^4, the free-free optical depth is unity at a frequency of $\nu_{ff} \gtrsim 10 f^{0.95}$ GHz (see Spitzer, 1978).

If we assume that the source advance speed is similar to the component expansion speed, the overall size of $\sim$ 7 pc, implies an age t$> 3 \times 10^3$ yr. This lower limit on the age is in agreement with the age estimated for typical "compact double" (Phillips & Mutel 1982; Hodges & Mutel 1987) or Compact Symmetric Objects (CSO) (Conway et al. 1994, Wilkinson et al. 1995) as "compact double" have been renamed when high sensitivity VLBI images revealed more morphological details in many former doubles. However, compact doubles or CSO's are one or two orders of magnitude larger in size than OQ 208, thus OQ 208 may be more strongly confined than typical CSOs, or if the CSO ages have been underestimated, OQ 208 could be a 'young' CSO.

On the other hand if the outward advance speed of the plasmoids is higher than the limit on the expansion velocity estimated before, from the ram pressure argument we obtain a lower limit for the particle density and a radio source age shorter than previously calculated. This will avoid the need of introducing free-free absorption and will strengthen the hypothesis that OQ 208 is a young CSO.

The optical image of the galaxy has an axial ratio of 0.7 corresponding, assuming a disk galaxy, to an inclination of $\sim 45^\circ$ with respect to the plane of the sky. If we assume that the radio axis is along the optical axis, the inclination of the jet is 45° also and the bulk velocity required to give a flux density ratio between the two regions (A/B and C/D) of about 10 via Doppler boosting is $\sim 0.5c$.

However, the lack of strong short time scale variability makes difficult to explain the difference in flux density between the two regions in terms of Doppler boosting. Intrinsic asymmetries may exist and are found in Compact Steep Spectrum (CSS) radio sources (Saikia et al. 1995). Indeed the radiative efficiency may be increased if a jet encounters a dense cloud, hence the difference in flux density may well reflect different ambient conditions at the two sides of the central Active Galactic Nucleus (AGN) or just random differences between the path of the jets.

5. Conclusions

The lack of flux density outbursts (and the presence of slow monotonic decrease at high frequency), the simple peaked spectral shape, and the double morphology are in contrast with the core-jet hypothesis proposed by Zhang et al. (1994) or the highly curved jet morphology (Charlot 1990). Despite the large ratios of the flux density of the components, OQ 208 is most likely a member of the "compact double" or CSO class of radio sources. We suggest that the NE and SW emitting regions are microlobes or even hot-spots embedded in the central region of the host galaxy, and confined by ram pressure in a dense medium that prevents or slows down the expansion into the interstellar and intergalactic medium.

It is interesting to note that OQ 208 is one of the most luminous far-infrared (FIR) radio sources (Mazzarella et al. 1991). The strong infrared emission, if not produced by the core requires a large amount of dust, estimated to be $\sim 5 \times 10^8 M_\odot$ around the central object (Knapp et al. 1990). This is consistent with the hypothesis of strong confinement by a high density environment. We note that the IR fluxes given by Mazzarella et al. (1991) and Knapp et al. (1990) differ substantially at 12 and 25 μm and are barely consistent at 60 and 100 μm. This is likely to be due to confusion, as reported by Mazzarella et al. (1991) for their published IR flux density measurements for this source.

Our hypothesis could be confirmed by the detection of a radio core between the two regions A/B and C/D in Fig. 3, very weak or hidden at cm wavelengths. A good set of high resolution and high sensitivity radio data are necessary to carry out a proper verification. EVN 22 GHz observations are planned for this purpose. The confirmation of our microlobe interpretation would mean that OQ 208 is the smallest compact double observed so far.

Acknowledgements. C.S. wishes to thank the STScI for providing support for his visit. M.B. and D.D. acknowledge financial support from the European Union as EU fellows under contract ERBCHBGCT920212. The WSRT is operated by the Netherlands Foundation for Research in Astronomy with the financial support of the Netherlands Organization for Scientific Research (NWO). The NRAO is a facility of the National Science Foundation operated under cooperative agreement by Associated Universities, Inc. The authors wish to thank an anonymous referee for helpful comments and suggestions.

References

Bicknell, G. V., Dopita, M. A., & O'Dea, C. P., 1996, in proceedings of IAU Symposium No. 175, Extragalactic Radio Sources, R.D. Ekers, C.Fanti & L.Padrielli eds, in press

Bondi M., Mantovani F., Sherwood W., Tzioumis A., Venturi T., 1994, A&AS, 103, 365

de Bruyn, A. G., 1990a, in Proc. Dwingeloo Workshop, Compact Steep Spectrum and GHz Peaked Spectrum Radio Sources, ed. C. Fanti, R. Fanti, C. P. O'Dea, & R. T. Schilizzi, (Bologna: Istituto di Radioastronomia), p206

de Bruyn, A. G., 1990b, in W.J. Duschl, S.J. Wagner & M.Camenzind (eds) Lecture Notes in Physics 377, Variability of Active Galaxies, Heidelberg, Germany, p105

Burbidge E.M., Strittmatter P.A., 1972, ApJ, 172, L37

Charlot P., 1990, A&A, 229, 51

Condon J.J., 1992, ARA&A, 30, 575

Conway J.E., Myers S.T., Pearson T.J., Readhead A.C.S., Unwin S.C., Xu W., 1994, ApJ, 425, 568

Dallacasa, D., Fanti, C., Fanti, R., Spencer, R.E., Schilizzi, R.T., 1995, A&A, 295, 27

Granato G.L., Zitelli V., Bonoli F., Danese L., Bonoli C., Delpino F., 1993, ApJS 89, 35

Hodges M.W., Mutel R.L., 1987, in *Superluminal Radio Sources*, eds. J.A. Zensus and T.J. Pearson, p168

Knapp G.R., Bies W.E., van Gorkom J.H., 1990, AJ 99, 476

Kühr, H., Witzel, A., Pauliny-Toth, I.I.K., Nauber, U., 1981, A&AS, 45, 367

van der Laan, H., Zieba, S., Noordam, J.E. 1984, IAU Symposium 110, VLBI and Compact Radio Sources, R.Fanti, K.I. Kellermann and G. Setti eds, Reidel, Dordrecht, p. 9

Marscher, A.P. 1977, ApJ, 216, 244 Marziani P., Sulentic J.W., Calvani M., Perez E., Moles M., Penston M.V. 1993, ApJ, 410, 56

Matveenko, L.I., Kostenko, V.I., Papatsenko, A.Kh., Bartel, N., Massi, M., Romney, J.D., Weiler, K.W., Ficarra, A., Mantovani, F., Padrielli, L., Moiseev, I.G., Bååth, L.B., Nicolson, G.D. 1981, Sov. Astron. Lett., 7, 259

Mazzarella J.M., Bothun G.D., Boroson T.A., 1991, AJ 101, 2034

Murphy, D.W., 1988, PhD Thesis, Univ. of Manchester

O'Dea C.P., Baum S.A., Stanghellini C., 1991, ApJ, 380, 66

Owen, F.N., Spangler, S.R., Cotton, W.D., 1980, AJ, 85, 351

Pacholczyk A.G., 1970, Radio Astrophysics, Freeman & C., S. Francisco

Perley, R.A., 1982, AJ, 87, 859

Phillips, R. B., & Mutel, R. L., 1982, A&A, 106, 21

Rusk, R.E., 1988, PhD Thesis, Univ. of Toronto

Saikia, D.J., Jeyakumar, S., Wiita, P.J., Sanghera, H.S., Spencer, R.E., 1995, MNRAS, 276, 1215

Spitzer, L., Jr., 1978, Physical Processes in the Interstellar Medium, John Wiley & Sons, New York

Stanghellini, C., Baum, S.A., O'Dea, C.P., Laurikainen, E., 1993, ApJ, 88, 1

Waltman E.B., Fiedler R.L., Johnston K.J., Spencer J.H., Florkowsky D.R., Josties F.J., McCarthy D.D., Matsakis D.N., 1991, ApJS, 77, 379

Wilkinson, P.N., Polatidis, A.G., Readhead, A.C.S., Xu, W., Pearson, T.J., 1995, ApJ, 432, L87

Zensus, J.A., Porcas, R.W., Pauliny-Toth, I.I.K. 1984, A&A, 133, 27

Zhang, F.J., Bääth L.B., Spencer R.E., 1994 A&A, 281, 649

This article was processed by the author using Springer-Verlag LaTeX A&A style file *L-AA* version 3.